ELSEVIER

Contents lists available at ScienceDirect

Chemical Geology

journal homepage: www.elsevier.com/locate/chemgeo



Research Paper

Vapor-liquid and liquid-liquid phase equilibria in the CO₂-CH₄-N₂ system: A Gibbs ensemble Monte Carlo simulation

Zhenhao Duan*, Nanfei Cheng

Department of Experimental Study under Deep-sea Extreme Conditions, Institute of Deep-Sea Sciences and Engineering, Chinese Academy of Sciences, Sanya, Hainan 572000, China

ARTICLE INFO

Editor: Claudia Romano

Keywords: CO₂-CH₄-N₂ Phase equilibria Gibbs ensemble Monte Carlo Computer simulation Natural gas

ABSTRACT

CO2, CH4, and N2 are the most common gaseous species in geological fluids, originating from diverse sedimentary, metamorphic, igneous, and hydrothermal processes. Analyzing relic paleo-geofluids trapped in minerals as fluid inclusions is crucial for understanding their roles in these geological processes, which depends on the established phase and volumetric behavior of the fluids as a function of pressure (P), temperature (T), and composition (x). However, collecting comprehensive data for such a ternary system across all potential PTx variables is a significant experimental challenge. Therefore, this study simulated the fluid-phase equilibrium in the unary, binary, and ternary systems of CO₂-CH₄-N₂ using the Gibbs Ensemble Monte Carlo (GEMC) method, a powerful molecular simulation technique for studying systems with multiple fluid phases. The considered PT range encompasses liquid/liquid, liquid/vapor, and liquid/liquid/vapor equilibrium regions. Molecular interactions in the system are described using two-body Lennard-Jones potentials, requiring only two temperatureindependent parameters for similar molecules. The Berthelot-Lorentz rules are applied to define the Lennard-Jones interactions for dissimilar molecules, with an additional temperature-independent mixing parameter. The equilibrium compositions and molar volumes of the coexisting phases in all mixtures are predicted with an accuracy comparable to that of the experimental data. The PT dependence of liquid-liquid-vapor coexistence at very low temperatures and the potential for gas-gas coexistence at high temperatures are discussed for the binary subsystems. It can be concluded that the GEMC simulation is an important "computational experiment" to investigate thermodynamic properties of natural fluids if molecular interaction potential is well described, providing appreciable supplementation to experimental findings.

1. Introduction

Substantial progress has been made in tracing the formation conditions and evolution of rocks, ore deposits, and oil and gas reservoirs by analyzing relic fluids trapped in minerals (e.g., Roedder, 1984; Samson et al., 2003; Chi and Steele-Mcinnis, 2024). Most fluids encountered in geochemical applications can be well represented by compositions in the system salt-CO₂-CH₄-N₂-H₂O. Consistent with this, gas chromatography and Raman laser probe analysis have shown that the non-aqueous phases in many fluid inclusions can be represented by binary or ternary mixtures in the CO₂-CH₄-N₂ system (e.g., van den Kerkhof, 1990; Seitz et al., 1994; Thiéry et al., 1994a; Le et al., 2020; Sublett et al., 2021). Despite the availability of techniques such as laser Raman microprobe spectroscopy (e.g., Le et al., 2020; Sublett et al., 2021; Chen and Chou, 2022; Zhang and Chou, 2024), micro-thermometry, which is

based on the temperature measurements at phase transitions in response to heating and cooling, remains a basic tool for analyzing the pressure, temperature, composition, and phase state of fluid inclusions at the time of entrapment (e.g., Roedder, 1984; Chi and Steele-Mcinnis, 2024). To utilize such analysis for extracting formation conditions from the determined compositions, it is essential to understand the phase and volumetric behavior of these fluids as a function of temperature (T), pressure (P), and composition (x).

Furthermore, the natural gas industry has shown increased interest in the $\rm CO_2\text{-}CH_4\text{-}N_2$ system. Despite substantial variation in natural gas composition, most gas resources contain significant amounts of carbon dioxide and nitrogen, in addition to methane and some other hydrocarbons (e.g., Faramawy et al., 2016). An enhanced understanding of phase equilibrium in this system could improve the recovery of methane and ethane through cryogenic processing (e.g., Al-Sahhaf et al., 1983; Li

E-mail address: zduan@idsse.ac.cn (Z. Duan).

^{*} Corresponding author.

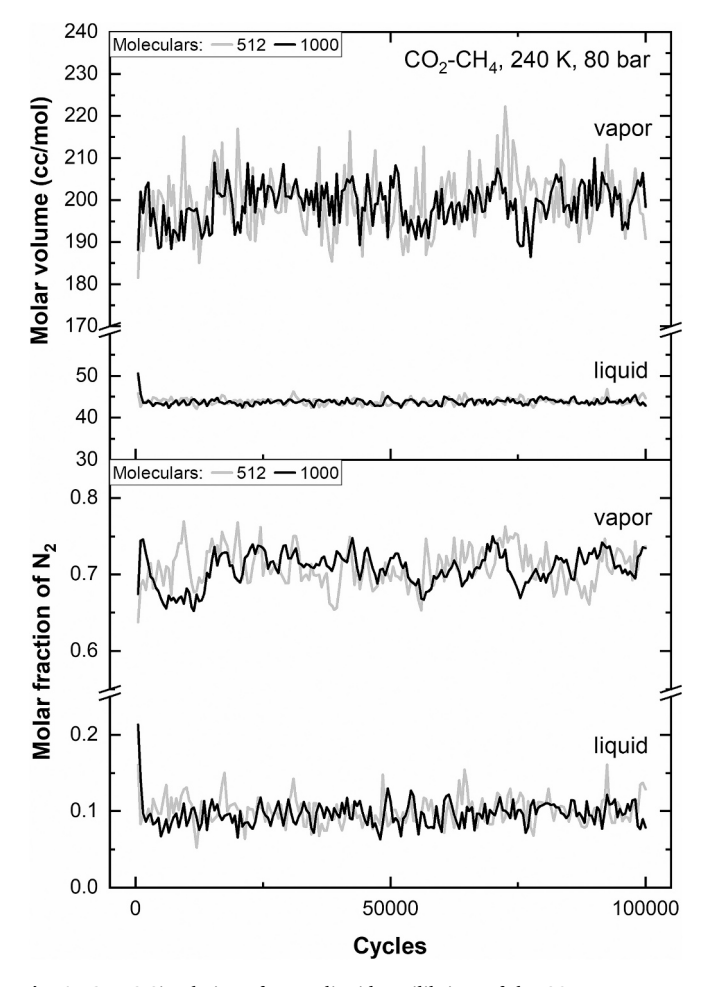


Fig. 1. GEMC Simulation of vapor-liquid equilibrium of the $\rm CO_2\text{-}N_2$ system at 240 K and 80 bar, using 512 vs. 1000 molecules, yielding very close vapor-liquid equilibrium densities and compositions.

et al., 2012).

While complete data sets and highly accurate equations of state (EOS) are available for the pure CO2, CH4, and N2 systems (Wagner and Span, 1993; Span and Wagner, 1996), experimental measurements of phase coexistence properties of mixtures (e.g., compositions and densities of coexisting phases) for these commonly encountered systems are generally limited to a narrow PTx range. Collecting data for a ternary system for all possible compositions, temperatures, and pressures required for interpretations would necessitate an enormous experimental effort. To address the challenge of expanding the region of application and interpolating between measurements, appreciable efforts have been devoted to developing accurate functional representations EOS of *PVTx* and phase coexistence properties. These EOS, such as those based on hard sphere fluids (e.g., Gubbins, 1985; Poling et al., 2001; Duan et al., 2003), may have some theoretical basis but ultimately contain many terms and parameters that are justified solely by their ability to fit the data. Because they are fitted to a limited range of data, their extrapolation beyond the range generally remains unproved. For mixtures, due to the increased dimensionality and limited data, the problem is more challenging. Popular cubic EOS with few parameters, such as the Peng-Robinson or Redlich-Kwong-Soave equations, can be extended to mixture equations with ease and can predict equilibrium compositions for mixtures with reasonable accuracy for non-aqueous systems (Thiéry et al., 1994a, 1994b; Thiéry and Dubessy, 1996; Mao et al., 2010; Zhang et al., 2023a). However, they generally exhibit large density errors up to 20 % or more. Given sufficient data, EOS for binary mixtures can be developed to make satisfactory predictions, although much less accurately than for pure systems (e.g., Wagner and Span, 1993; Span and Wagner, 1996). An example is the EOS for the binaries developed by Duan et al. (1996, 2000). However, describing thermodynamic properties in the critical region is fundamentally difficult by using conventional EOS functionalities (Jin et al., 1993; Kiselev and Friend, 1999), necessitating special behavior additions for reliable predictions.

An alternative to using EOS for interpolation and extrapolation is to compute thermodynamic properties through computer simulations based on assumed or calculated molecular-level interactions. As computational power continues to increase, molecular dynamics (MD) and Monte Carlo (MC) simulations have become promising methods to address the limitations of EOS in terms of data and functionality. For instance, MD simulations of thermodynamic properties under extreme conditions, such as those in the deep crust and mantle, have been documented (e.g., Brodholt and Wood, 1990; Belonoshko and Saxena, 1991; Duan et al., 2000; Zhang and Duan, 2005; Yang et al., 2017).

This paper presents the results of phase equilibrium simulations for the $\rm CO_2\text{-}CH_4\text{-}N_2$ system using the Gibbs Ensemble Monte Carlo (GEMC) method with a Lennard-Jones (LJ) representation of intermolecular interactions (Panagiotopoulos, 1987, 1992, 2000; Duan et al., 2004; Zhang et al., 2023b). Despite the simplicity of this representation, which involves only a few temperature-independent parameters (two for each unary interaction and one additional for each binary interaction), the results for binary and ternary systems closely match experimental data and are significantly more accurate than those obtained from even highly parameterized EOS in certain PT ranges. This is particularly true for the critical region, where conventional EOS approaches fail to accurately represent mixture data in the critical range. A primary objective of this research is to showcase the GEMC method as an efficient "computational experiment" for studying natural fluids.

2. Description of the VLE simulation

The GEMC method, introduced by Panagiotopoulos and colleagues (e.g., Panagiotopoulos, 1987; Panagiotopoulos et al., 1988), is considered the most efficient and accurate approach for simulating vapor/liquid equilibria (VLE). Consequently, this method has been extensively utilized in different fields, including the energy and chemical industries (e.g., Sadus, 1999; Li et al., 2012; Henley and Lucia, 2015). However, its potential applications in Earth and planetary science remain to be further explored (Zhang et al., 2023b). For a comprehensive description of the method and its improved algorithms, see Panagiotopoulos (1992, 2000) and Zhang et al. (2023b).

In our simulations, 512 molecules were distributed between the vapor box and liquid box to achieve the desired binary or ternary total composition. Increasing the particle number from 512 to 1000 showed little difference in our results, as shown in Fig. 1. The total number of molecules, the total volume of the two simulation boxes, and the temperature were kept constant throughout the simulation. The initial structure of the system was based on a face-centered cubic lattice. Random exchanges (approximately twice the total number of molecules) of the initial positions of different components helped reduce the preequilibrium time. The initial allocation of molecules between the two simulation boxes must satisfy two key criteria: (1) The total composition should be within the two-phase region, rather than in the homogeneous region; and (2) At least 100 molecules must remain in each box after the system reaches equilibrium. If too many molecules accumulate in one phase, the initial setup should be adjusted accordingly. The simulation was conducted using three types of moves (Panagiotopoulos, 1987): (1) random molecule displacements within each box to ensure equilibration within a single phase; (2) adjustments in the volumes of the two regions to equalize the average pressures in the coexisting phases; and (3) random transfers of molecules between phases to equalize the chemical potential of similar components in the two phases (Panagiotopoulos, 1987). Volume change attempts were selected from a uniform

Table 1 L-J potential parameters in Eq. (1).

Component	ε (Κ)	σ (Á)
CO ₂	247.0	3.69
CH ₄	147.9	3.73
N_2	101.0	3.63

Table 2
Mixing parameters in Eqs. (2) and (3).

Binary	K _{1,ij}
CH ₄ -CO ₂	0.91
CH ₄ -N ₂	0.9221
N ₂ - CO ₂	0.9003

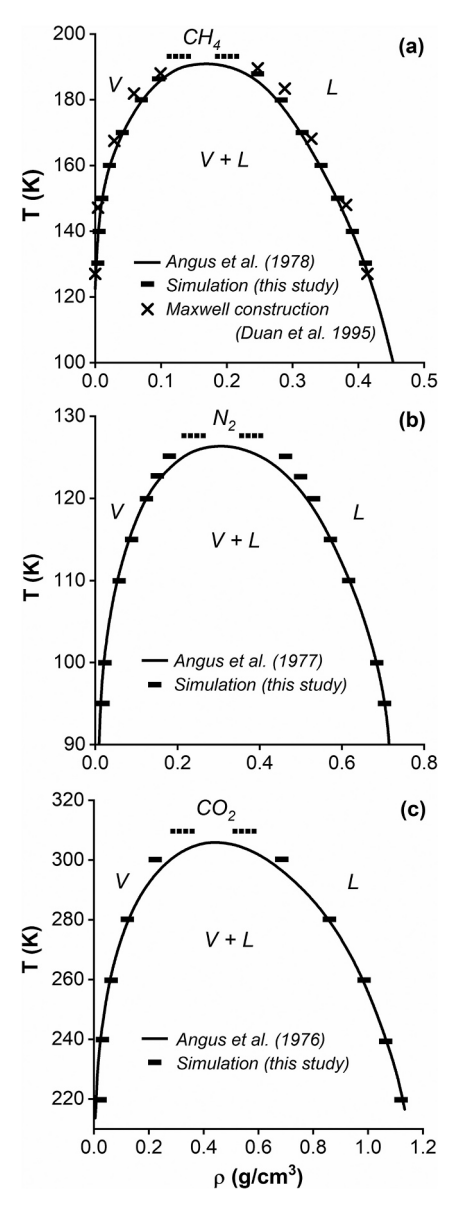


Fig. 2. The density of the coexisting phases of the pure systems (a) CH_4 , (b) N_2 , and (c) CO_2 .

distribution. The maximum volume change was adjusted during the run to achieve an acceptance ratio of 50 %. In a cycle following steps 1 and 2, the supplying and receiving boxes were chosen at random, and a random

Table 3Triple and critical points of pure systems.

Triple point		Critical point(exp.)	Critical point (GEMC)	
CO ₂	216.58 K, 5.185 bar	304.21 K, 73.825 bar	318.0 K, 77.0 bar	
CH ₄	90.68 K, 0.117 bar	190.555 K, 45.95 bar	193.8 K, 46.8 bar	
N ₂	63.148 K, 0.125 bar	126.20 K, 34.00 bar	130.0 K, 35.1 bar	

species in the supplying box and a random position in the receiving box were selected. The energy change due to removing a molecule from the supplying box and inserting it into the receiving box was calculated, and the move was accepted or rejected based on a Boltzmann criterion as described in the Panagiotopoulos review (Panagiotopoulos, 1992). The low acceptance rate of insertions becomes problematic at high densities. To increase this rate, we employed the inflating flea method (Pablo and Prausnitz, 1989) in the simulation of liquid-liquid phase equilibria and the search for an upper critical phase separation (gas-gas equilibria) at high pressures.

The aforementioned three types of move constitute a single cycle. Typically, each cycle comprises approximately 2000 (3 or 4 times the number of molecules) attempted molecular displacements, 1–2 attempted volume changes, and 50–200 attempted particle interchanges. To achieve reliable statistics, the simulations were continued until there were approximately 5000 successful interchanges for each species. Generally, 10,000 cycles of pre-equilibrium followed by 20,000 cycles of data collection were required. The number of successful interchanges decreases substantially with decreasing temperatures. Consequently, more cycles and special insertion steps (Pablo and Prausnitz, 1989) were necessary for temperatures below 240 K.

The interactions between all molecules were described by LJ potentials of the formula,

$$U_{ij} = 4\varepsilon_{ij} \left[\left(\frac{\sigma_{ij}}{r_{ij}} \right)^{12} - \left(\frac{\sigma_{ij}}{r_{ij}} \right)^{6} \right]$$
 (1)

where ε_{ij} and σ_{ij} are the energy and size parameters and r_{ij} is the distance between the centers of the two molecules. we selected cut-off distances equal to half the length of the respective simulation boxes. Given that the length of each simulation box is at least three times the size parameter σ , the resulting cut-off energy is significantly less than 1 %. The Berthelot-Lorentz rules,

$$\varepsilon_{ij} = k_{1,ij} \sqrt{\varepsilon_i \varepsilon_j} \tag{2}$$

and

$$\sigma_{ij} = \left(\sigma_i + \sigma_j\right)/2\tag{3}$$

were utilized to determine the parameters for interactions between dissimilar species based on parameters for similar species. $k_{1,ij}$ is a temperature-independent parameter, which was adjusted to enhance agreement with mixed system data. $k_{1,ij}$ and other parameters for the $N_2\text{-}CH_4$ and $CO_2\text{-}CH_4$ binaries were derived from our previous simulations of these mixtures in the supercritical region (Duan et al., 1996, 2000). These simulations described the measured behavior of these gases up to 2000 K and 100,000 bar, demonstrating the extensive range of temperature and pressure that can be captured by this simple parameterization. To improve the agreement with the VLE data discussed here, the parameters for the $CO_2\text{-}CO_2$ and $N_2\text{-}CO_2$ interactions were slightly adjusted. This adjustment did not affect the accuracy of the volumetric simulations. They are summarized in Tables 1 and 2.

Just like in experiments, the initial setup is crucial for a successful simulation. If the initial total composition of both simulation boxes lies within a homogeneous region or outside the two-phase region, it is impossible to achieve two-phase equilibrium at the given temperature and pressure. Therefore, the optimal setup is to allocate about an equal number of molecules in the two boxes. If this approach is unsuccessful,

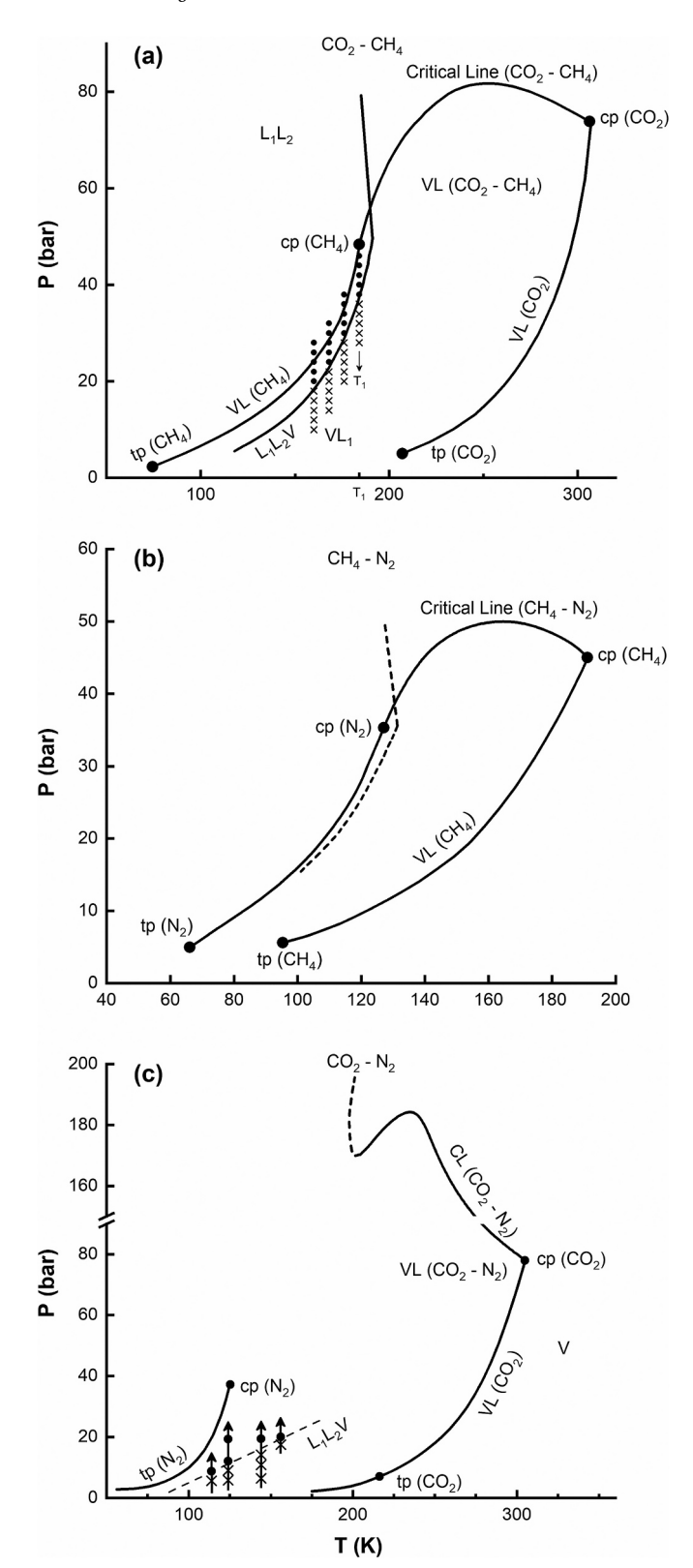


Fig. 3. The PT projection of the systems (a) $\rm CO_2\text{-}CH_4$, (b) $\rm CO_2\text{-}N_2$, and (c) $\rm CH_4\text{-}N_2$.

the initial setup should be adjusted based on the final configuration of the previous run.

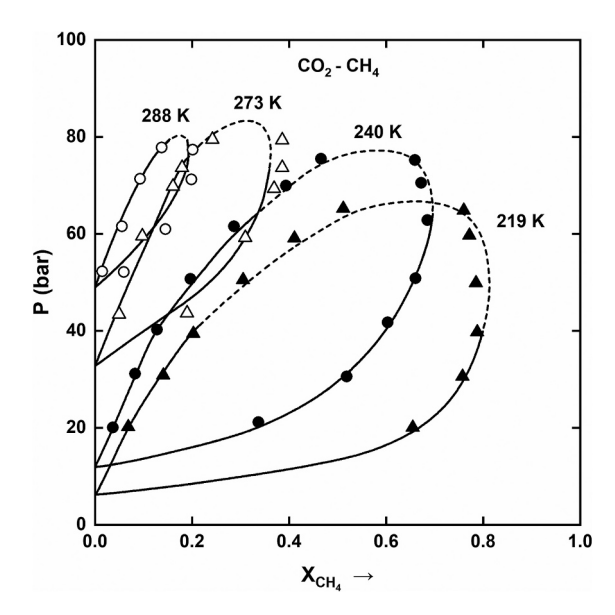


Fig. 4. The phase equilibria of the $\rm CO_2\text{-}CH_4$ system at various temperatures (simulated results vs. experimental data. The symbols are simulated results of this study, and the solid lines represent smoothed data of Arai et al. (1971) and Al-Sahhaf et al. (1983).

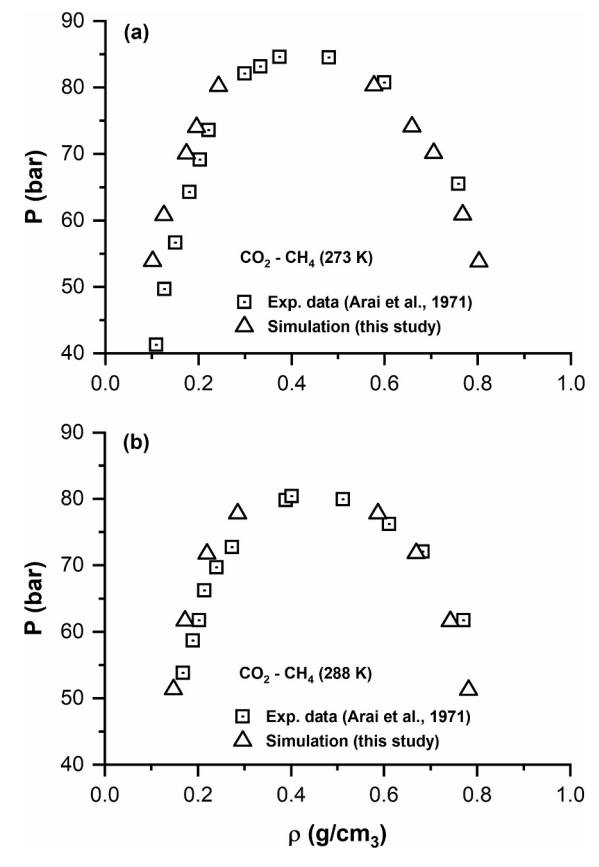


Fig. 5. Comparison of the simulated densities of the systems (a) $\rm CO_2\text{-}CH_4$ and (b) $\rm CO_2\text{-}N_2$ with the experimental data of Arai et al. (1971).

3. Results and comparison with experimental data

3.1. Pure systems

In a previous publication (Duan et al., 1995), we reported

Table 4 Simulated phase equilibrium results in the system ${\rm CO_2\text{--}CH_4}$ in the liquid-liquid-vapor equilibrium region.

T(V)		vLl	vL2(or:V)	V ^{L1} (cm ³ /mol)	V ^{L2(or:V)} (cm ³ /mol)
T(K)	P(bar)	X _{CO2}	X _{CO2} ^{L2(or:V)}		
160	14	0.895	0.0128	36.52	593.8
160	15	0.950	0.035	35.30	47.21
160	24	0.956	0.063	35.34	46.15
160	26	0.951	0.058	35.22	46.08
160	32	0.962	0.078	35.11	45.7
170	5	0.982	0.215	36.9	2676.4
170	22	0.959	0.034	36.90	478.6
170	23	0.944	0.029	37.04	390.6
170	24	0.951	0.071	36.23	49.49
170	30	0.945	0.075	36.18	49.51
170	33	0.946	0.091	36.11	49.1
170	50	0.950	0.11	36.24	47.7
170	100	0.95	0.11	35.96	45.70
170	200	0.96	0.16	35.2	42.65
180	5	0.982	0.337	38.2	2840.0
180	12	0.98	0.145	38.0	1108.9
180	18	0.972	0.097	38.0	692.7
180	22	0.98	0.084	37.50	536.2
180	30	0.951	0.051	37.82	326.2
180	31.6	0.945	0.048	37.6	315.7
180	31.7	0.940	0.040	37.6	55.0
180	33	0.941	0.046	37.18	54.8
180	37	0.933	0.083	37.16	54.6
180	42	0.932	0.099	37.2	53.3
180	100	0.941	0.123	36.6	48.3
180	200	0.932	0.125	36.5	44.8
180	300	0.940	0.251	36.1	41.9
185	30	0.962	0.074	38.22	366.9
185	35	0.950	0.062	38.31	281.7
185	38	0.930	0.053	37.6	255.0
185	42	0.930	0.091	37.57	58.92
190	5	0.980	0.442	39.5	3011.1
190	18	0.981	0.199	38.6	755.3
190	35	0.92	0.074	38.7	140.5
190	40	0.95	0.083	38.5	239.7
190	50	0.914	0.091	38.2	62.8
190	60	0.91	0.110	38.2	58.7
190	80	0.91	0.115	37.9	54.9
190	120	0.92	0.152	37.7	50.2
190	200	0.91	0.131	37.3	46.9
190	300	0.931	0.384	36.9	42.11
200	10	0.978	0.651	38.5	1584.0
200	30	0.962	0.320	38.2	553.0
200	50	0.940	0.11	39.7	187.7
200	60	0.892	0.091	40.1	100.9
200	70	0.874	0.109	40.0	67.9
200	100	0.92	0.17	38.7	56.03

The numbers in the parentheses are the uncertainties in the simulation. L_1 : CO_2 rich liquid; L2: CH_4 rich liquid.

simulations of VLE of the end member systems CO_2 , CH_4 , and N_2 . These calculations were based on extensive molecular dynamics simulations of the PVT properties of the CH_4 system. The simulated PVTx data were fit to an EOS and the phase equilibria were found from a Maxwell construction. This model of the CH_4 system was then successfully used to predict the VLE of N_2 and CO_2 through a scaling argument based on the LJ parameters of the system of interest.

In this article, the GEMC method is used to directly calculate VLE for the end members. This method provides the equilibrium densities of coexisting phases for a given temperature in a single simulation. In Fig. 2a, we present both the prior results obtained using Maxwell construction and the new results derived from the GEMC simulations for the CH₄ system. Below the critical region (e.g., $T < 170~\rm K$), the GEMC results (depicted as bars) are in good agreement with the models of Angus et al. (1976, 1978), which have been widely recognized for its accurate representation of experimental data and has been recommended by IUPAC. Within the non-critical region (below approximately 170 K), the GEMC results appear to be more accurate than those obtained from MD simulations combined with Maxwell construction (depicted as crosses). This

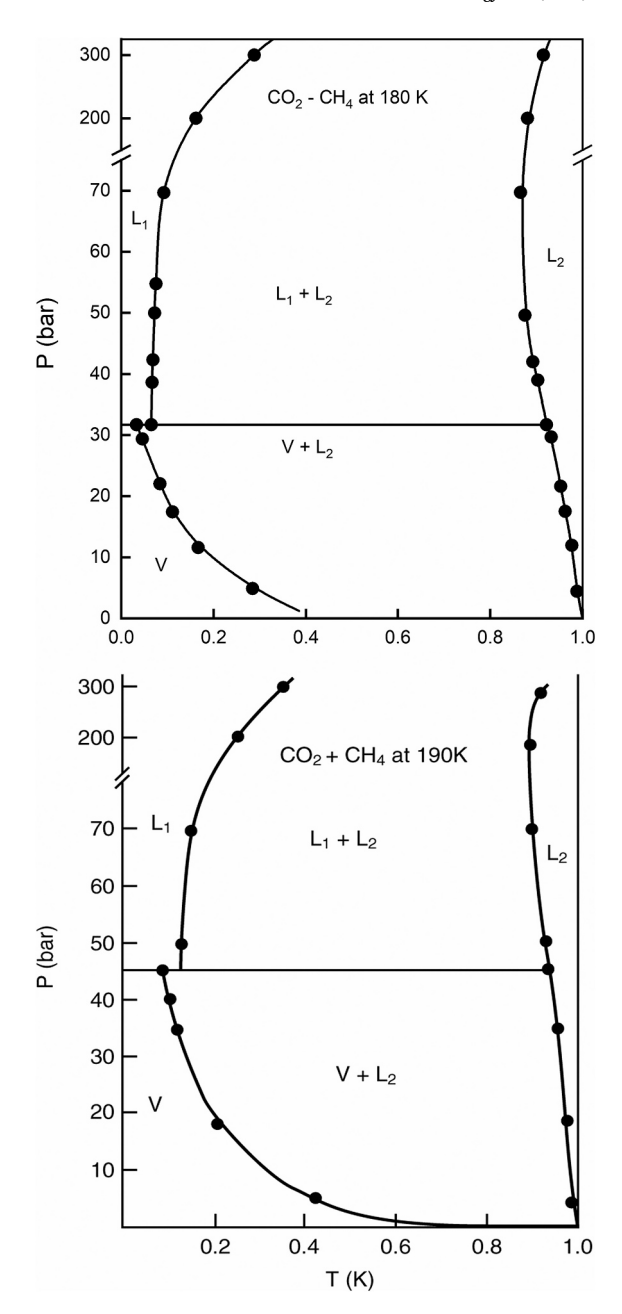


Fig. 6. Schematic of the isothermal composition pressure projections in the CO_2 - CH_4 system at (a)180 K and (b) 190 K.

discrepancy arises because, in the earlier work, the *PVT* simulation results were fitted to an EOS. Despite the large number of parameters involved, the EOS does not adequately represent the critical region. This is a common challenge associated with EOS methods. The GEMC method also exhibits similar limitations. In the critical region, results from the GEMC method become unstable, akin to experimental measurements, making it difficult to precisely identify the critical point.

To obtain approximate estimates of the critical parameters, extrapolation methods must be used (see below). Results for the N_2 and CO_2 systems are presented in Fig. 1b and c. The simulated critical densities, pressures, and temperatures of the pure systems are compared to the measured values in Table 3. To estimate the density and temperature coordinates of the critical point, the coefficients of the truncated Wegner (Wegner, 1972) expansion were used,

$$|\rho_l - \rho_v| = A_1 (T_c - T)^{\beta} + A_2 (T_c - T)^{\beta/2}$$
(4)

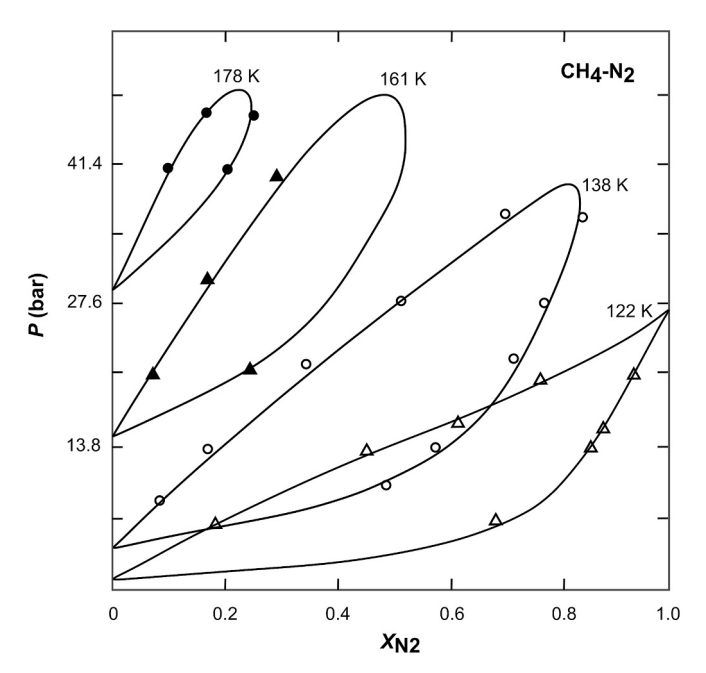


Fig. 7. Coexisting phase compositions for the $\mathrm{CH_{4}\text{-}N_2}$ system as a function of temperature, with curves smoothed from the experimental data of Stryjek et al. (1974) incorporated for comparison.

where $\beta=0.325$, were adjusted to fit the difference simulated densities of the coexisting phases at several temperatures in the critical region. The critical densities were calculated by fitting the density to the law of rectilinear diameter (Ley-Koo and Green, 1981).

$$\frac{(\rho_l + \rho_v)}{2} = \rho_c + B(T - T_c) \tag{5}$$

The critical pressure was estimated by fitting the calculated saturation pressure versus temperature data to the Antoine equation (Poling et al., 2001) and extrapolating to the critical temperature. The critical parameters summarized in Table 3 show approximate agreement with the measured values. This agreement is better than what would be obtained from Maxwell constructions using highly parameterized EOS approaches (as shown in Fig. 2a). It is noteworthy that this accuracy is achieved without any special adjustments to the model in the critical region. This supports the application of the simulation method to the more challenging binaries and ternaries. The parameter $\beta=0.325$ was adjusted to fit the difference between simulated densities of the coexisting phases at several temperatures in the critical region. The critical densities were determined by fitting the density to the law of rectilinear diameter (Ley-Koo and Green, 1981).

3.2. Binary systems

Even for these commonly encountered binary systems, there is very limited experimental data, usually covering only a small part of the *PT* range needed for applications. While fairly simple EOS representations such as the Redlich-Kwong-Soave or the Peng-Robinson equations can provide quantitative representations of the VLE composition measurements, their predictions of the density of the mixtures are usually quite poor. In addition, since these EOS have little theoretical justification, their extrapolation beyond the range of the database is always questionable. As in the pure systems, the representation of binary data using an EOS is much worse in the critical region. On the other hand, in the GEMC methods used here, if the assumptions are accurate at the molecular level, the predictions of the simulation should be precise in regions where good statistics have been obtained. After conducting numerous repeated simulations in the critical region, we have concluded

that the GEMC method, similar to experimental measurements but superior to conventional EOS, encounters significant uncertainties in predicting critical properties.

The phase behavior of binary mixtures can be succinctly summarized by projecting the univariant lines in the *PTx* volume onto the *PT* plane. Fig. 3a and b illustrate the PT projections of the CO₂-CH₄ (2a) and CO₂-N₂ (2b) binary systems. These figures schematically represent the results of our simulations, as discussed in more detail below. However, similar to experimental data, they are derived from a limited number of simulations, and no effort has been made to interpolate the simulated data using an EOS. The GEMC method only allows for the simulation of fluid phases; therefore, only the phase relations between liquids, vapors, and supercritical fluids are shown. The triple point of the CO2 system is above the critical temperatures of the N₂ and CH₄ systems. Therefore, in Fig. 2a and b, we have illustrated the phase relations between the stable liquid phases and the extension of the CO₂ liquid line to temperatures below the CO₂ triple point. CO₂-rich fluids have not been observed in these binaries. However, such behavior has been inferred from microthermometry of fluid inclusions containing ternary mixtures (van den Kerkhof et al., 1993; Thiéry et al., 1994a).

Based on the calculated phase coexistence predicted from the van der Waals EOS, Van Konynenburg and Scott (KS) have presented a useful classification scheme for the *PT* projections (McGlashan and Schneider, 1978; van Konynenburg and Scott, 1980; Gubbins et al., 1983). As discussed in more detail below, the *PT* projection for the CO₂-CH₄ binary, Fig. 3a, shows it to be a class II system using KS notation. The CH₄-N₂ binary, illustrated in Fig. 3b, is a class I system, and the CO₂-N₂ system, depicted in Fig. 2c, is a class III system. It is difficult to directly simulate metastable liquid behavior even in this simple representation of the ternary fluid. Therefore, our results for these phase equilibria are restricted to the estimation of the binary behavior. However, this behavior is valuable for interpreting ternary fluid data (Thiéry et al., 1994a).

3.2.1. The CO₂-CH₄ binary

The simulation results of vapor-liquid coexistence for this system are compared to experimental data in Fig. 4. The results are consistent with the smoothed data of Arai et al. (1971) and Al-Sahhaf et al. (1983). The maximum and average deviations from the measured compositions are approximately $0.02\sim0.04$ in mole fraction, respectively, which are close to the experimental uncertainty. Generally, the largest deviations occur in the critical region, where the experimental uncertainty is also greatest.

EOS descriptions of mixed systems often accurately represent the compositions of coexisting phases but poorly describe the coexisting phase densities (Thiéry et al., 1994b). In Fig. 5a and b, the equilibrium densities from the simulations are compared to data (Arai et al., 1971). The average error is approximately 3.5 %, with the largest error being less than 10 %. This is much better than the errors of up to 30 % from the PR EOS or the SRK EOS (Soave, 1993; Thiéry et al., 1994b). These results also surpass those of the EOS by Lee and Kesler (1975) with errors up to 16 %, which provide more accurate densities than the PR EOS or the SRK EOS but less accurate coexisting phase compositions.

The PT projection for this system is given in Fig. 3a. The temperature at triple point of CO_2 is above the critical point of CH_4 . In our simulations, which do not allow the presence of a solid phase, the critical pressures on the vapor-liquid critical line first increase and then drop, suggesting that the critical line goes continuously from the critical point (cp) of CH_4 to the cp of CO_2 , which can be seen in Fig. 3a. An additional interesting binary phase coexistence appears at lower temperatures and pressures (i.e. the L_1L_2V line on Fig. 3a). Below the L_1L_2V line, CO_2 -rich liquid phase separates from vapor phase (L_1 -V). As pressure increases along an isotherm up to the L_1L_2V line, a CH_4 -rich liquid phase emerges, and the vapor phase vanishes. For example, as we simulate along the 180 K isotherm (see Table 4), if the pressure is below 31.7 bar, a CO_2 -rich liquid phase co-exists with a CH_4 -rich vapor phase. However, when

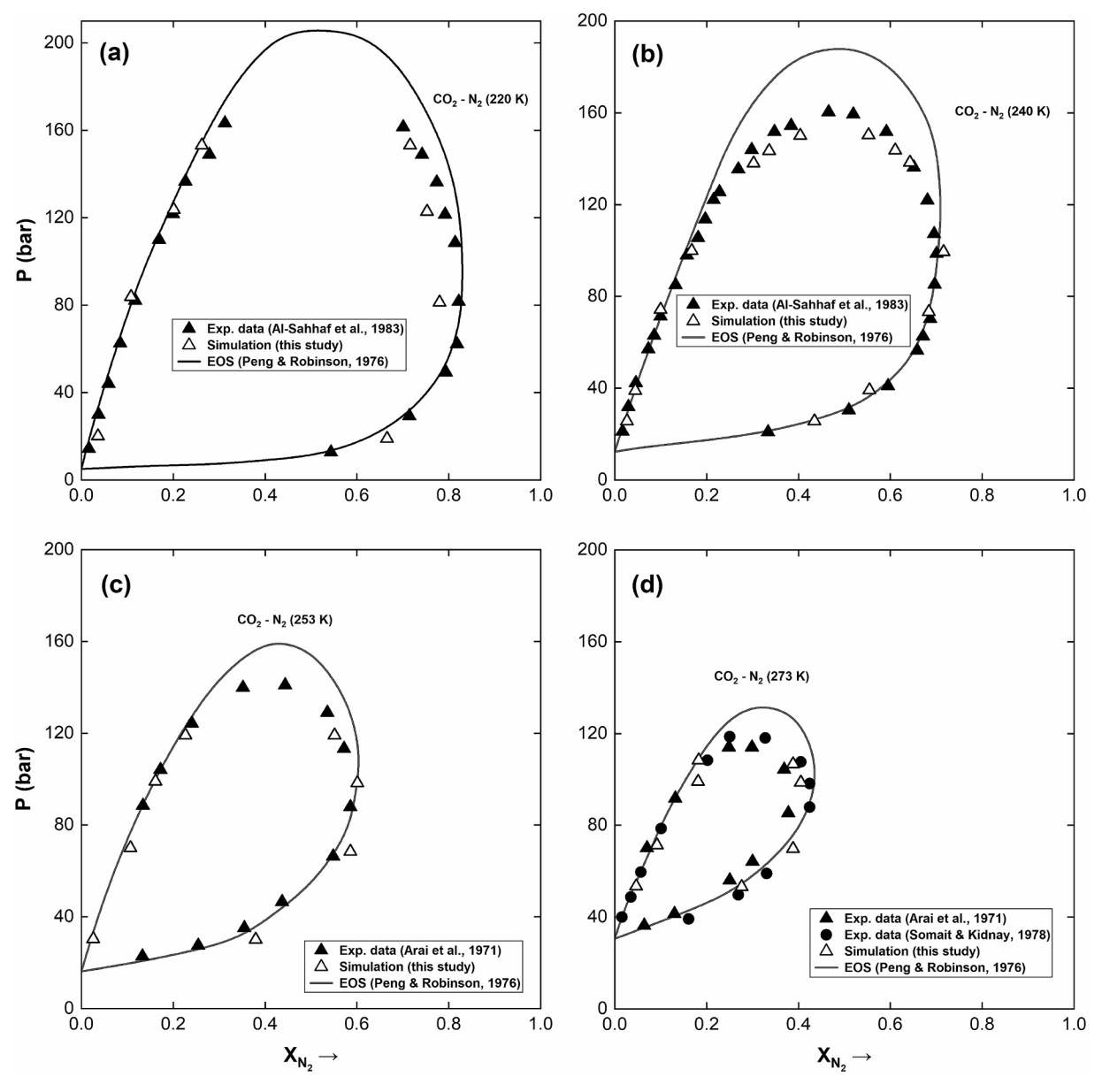


Fig. 8. The phase equilibria of the CO₂-N₂ system at (a) 220 K, (b) 240 K, (c) 253 K, and (d) 273 K with indicated experimental data and EOS curves for comparison.

we increase the pressure slightly up to 31.7 bar, the vapor phase is suddenly replaced by a liquid phase, the molar volume changes from 315.7 cm³/mol drops to 55 cm³/mole. There must be a liquid (CH₄ -rich)-liquid (CO₂-rich)-vapor three-phase equilibrium between 31.6–31.7 bar. A pressure-composition diagram along the T₁ isotherm in Fig. 3a is given in Fig. 6. The composition and transition temperatures appearing in this diagram were obtained from our simulations. As the pressure increases along the isotherm and approaches the saturation line of CH₄, the isotherm T₁ crosses the three-phase line (L₁L₂V line). Since for this system the liquid-vapor critical line extends from cp (CH₄) to cp (CO₂), the L₁L₂V line ends at an upper critical end point (UCEP). In Table 4, simulation results are presented for several isotherms that intersect the L₁L₂V line. Note the sharp decrease in density of the CH₄rich phase as the pressure is increased along the isotherm. Because of the low solubility of CO2 in the coexisting CH4 phase, it is very difficult to define the V₁-L₁ coexistence region. However, its general structure (illustrated in Fig. 6) may be inferred from the vapor composition just below the three-phase line, the saturation pressure of CH₄, and the composition of the composition of L₁ just after the three-phase line is

crossed. Examples of isotherms in this region are illustrated in Fig. 4. They all begin at the ${\rm CO_2}$ saturation line and form a continuous loop.

3.2.2. The N_2 -CH₄ binary

The cps of N_2 and CH_4 are quite close and the tp of CH_4 is at a lower temperature than the cp of N_2 (Table 3). Our simulated isotherms are compared to experimental data in Fig. 7. The agreement between the simulations and the data is impressive. Simulations and data show that for this binary there is a continuous line from the cp of CH_4 to the cp of N_2 . So far, we have not been able to identify a three $V-L_1-L_2$ line for this system. This would lead to a PT projection as in Fig. 3b leading to a KS classification as type II. It seems to be consistent with the available lowest temperature data (Stryjek et al., 1974). The data for 122 K suggests that the system is nearly an ideal solution. However, liquid-liquid simulations are difficult for this system because the low temperature makes it difficult to find successful insertion moves.

3.2.3. The N_2 -CO₂ binary

From Table 3 we see that the critical parameters for the endmembers

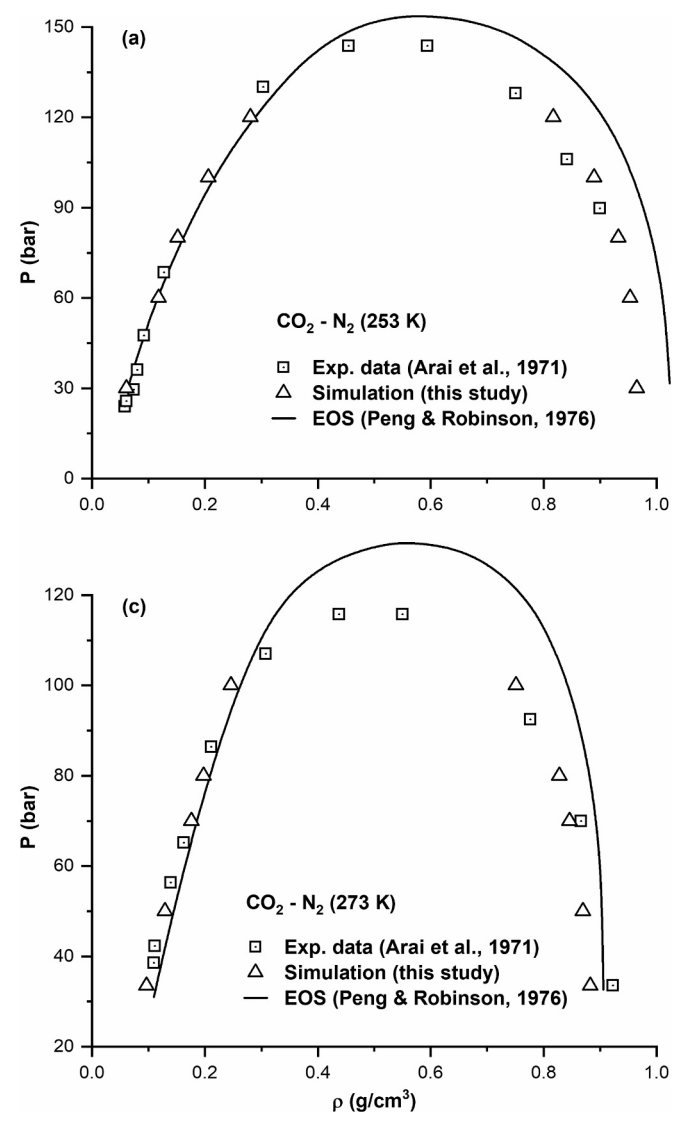


Fig. 9. Predicted coexisting phase densities for the ${\rm CO_2\text{-}N_2}$ binary system at (a) 253 K and (b) 273 K with indicated experimental data and EOS curves for comparison.

Table 5 Simulated phase equilibrium results in the system ${\rm CO_2\text{-}N_2}$ in the liquid-liquid-vapor equilibrium region.

T	P	X_{CO2}^{L1}	X ^{L2(or:V)}	V ^{L1} (cm ³ /	V ^{L2(pr:V)} (cm ³ /
(K)	(bar)			mol)	mol)
112	7	0.973(0.01)	0.09(0.01)	30.8(0.6)	1130.8(22.1)
112	10	0.87(0.012)	0.29(0.018)	32.5(0.7)	40.01(1.3)
112	20	0.76(0.013)	0.30(0.02)	31.2(0.6)	37.6(1.0)
123	7	0.98(0.015)	0.01(0.001)	31.10(0.8)	1333.3(22.2)
123	10	0.97(0.012)	0.01(0.001)	31.44(0.8)	910.9(9.2)
123	11	0.89(0.022)	0.26(0.018)	33.2(0.9)	40.43(1.1)
123	20	0.924	0.234	33.1(0.6)	39.50(0.8)_
		(0.012)	(0.020)		
145	7	0.98(0.1)	0.017	34.9(1.3)	1629.9(30.6)
			(0.002)		
145	10	0.96(0.01)	0.015	34.9(1.3)	1109(24.3)
			(0.003)		
145	20	0.93(0.017)	0.011	34.8(1.2)	515(14.5)
			(0.002)		
160	17	0.957(0.02)	0.14(0.01)	33.1(0.9)	687(18)
160	20	0.86(0.16)	0.29(0.013)	35.6(1.5)	44.6(1.8)

The numbers in the parentheses are the uncertainties in the simulation.

of this system have the largest separation of all the binaries in this ternary. Simulations and the current interpretation of the data (Thiéry et al., 1994a) lead to a PT projection, Fig. 3c, that is quite different from that of the CH₄-CO₂ and the CH₄-N₂ binaries. For this system, the critical line coming out of the CO2 cp moves to higher pressures for lower temperatures and shows no evidence of connecting to the cp of N₂ (type III according to van Konynenburg and Scott, 1980). The simulated vapor-liquid coexistence curves are compared to the available experimental data of Al-Sahhaf et al. (1983) and Arai et al. (1971) in Figs. 8a-d. The largest deviation is about 0.05 in mole fraction (except for the critical region), which is close to experimental uncertainty. The solid lines in the figures represent predictions from the frequently cited Peng-Robinson (PR) equation of state Peng and Robinson (1976). Note that in the critical region, these predictions are not very satisfactory. In Figs. 9a and b the densities of the coexisting phases in the CO₂-N₂ system are presented. Again, the simulated results are close to the experimental values (Arai et al., 1971). The largest error is about 10 %. The PR EOS (1976) provides relatively poor predictions for densities with errors as large as 8-30 % in this region.

The EOS calculations of Kreglewski and Kenneth (1983) predict that the critical line emerging from the cp of $\rm CO_2$ and moving to higher pressure as the temperature is lowered, see Fig. 3c, meets at a double critical point with a gas-gas critical line (dashed line) coming down from very high pressures. We did a lot of simulations in this region looking for a gas-gas critical line but could not find this behavior. Rather the liquidgas critical line continues to increase as the temperature is reduced as illustrated in Fig. 3c. This behavior is consistent with the results reported by Thiéry and Dubessy (1996) using EOS methods. As for the $\rm CO_2\text{-}CH_4$ binary, the simulations did find a $\rm VL_1L_2$ three-phase line. In Table 5 simulation $\rm \it PTx$ results are reported. We note a dramatic change in density as the pressure is increased along a constant temperature line (as in the $\rm CO_2\text{-}CH_4$ system) indicating a change of the $\rm N_2\text{-}rich$ phase from a vapor to a liquid density.

3.3. Simulations in the ternary

Knowledge of the *PVTx* behavior and phase coexistence in the full ternary is essential for the interpretation of formation conditions from the observed composition, density, and phase relations in fluid inclusions. Presently available EOS methods require a great deal of data for reliable application even to binary systems. Developing a ternary EOS is more difficult than for a binary (Thiéry et al., 1994b). On the other hand, in the GEMC approach presented here once having assumed two-body interactions at the molecular level, no additional assumptions are required to move from the binaries to the ternaries.

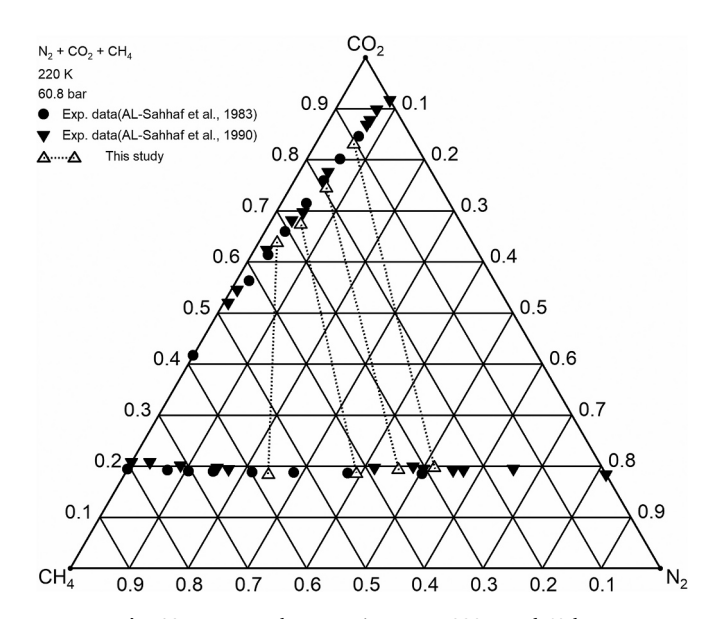
PVTx calculations in the ternary are straightforward. However, our present implementation of the GEMC simulation will not allow us to treat liquid-liquid phase equilibrium in dense ternary fluids (e.g. the metastable fluid coexistence range). Therefore, the phase coexistence simulations reported here are restricted to high temperatures and relatively low pressures. Results are reported for four temperatures (220 K, 240 K, 250 K, and 270 K) and various pressures in Table 6 and Figs. 10 and 11 (a-d). The agreement between the simulated estimates of the compositions of coexisting phases and the experimental data of Al-Sahhaf et al. (1983) is excellent.

Experimental volumetric data on the CO_2 - CH_4 - N_2 system are not available (van den Kerkhof, 1990). To provide estimates of volumes as a function of PTx for fluid inclusion analysis, Thiéry et al. (1994b) employed an approximate method that involved incorporating the molar amounts of N_2 into the CO_2 - CH_4 binary system or the molar amount of CH_4 into the CO_2 - N_2 binary system. The Peng-Robinson equation of state (PR EOS) was subsequently applied to determine phase coexistence and phase compositions, while the Lee-Kesler EOS was used to calculate the density. For instance, when estimating the properties of the N_2 - CO_2 - CH_4 ternary system using the CO_2 - CH_4 binary, they effectively assigned the N_2 to either the CO_2 or CH_4 component. This

Table 6
Simulated phase equilibrium results for the ternary system CO₂-CH₄-N₂.

T (K)	P (bar)	$X_{ m CO2}^{ m L}$	X_{CH4}^{L}	$X_{ m N2}^{ m L}$	$X_{\mathrm{CO2}}^{\mathrm{V}}$	$X_{\mathrm{CH4}}^{\mathrm{V}}$	$X_{ m N2}^{ m V}$	V ^L (cm ³ /mol)	V ^V (cm ³ /mole)
220	30	0.873(16)	0.108(15)	0.019(3)	0.288(8)	0.548(7)	0.164(2)	44.9(0.8)	511(24)
220	30	0.905(13)	0.065(13)	0.030(4)	0.310(12)	0.344(5)	0.346(8)	44.7(0.8)	522(15)
220	30	0.888(15)	0.101(15)	0.011(1)	0.282(17)	0.636(16)	0.082(3)	43.1(0.5)	520(25)
220	60	0.765(20)	0.155(15)	0.080(8)	0.203(13)	0.395(9)	0.402(9)	46.5(0.5)	231(8)
220	60	0.756(20)	0.159(18)	0.085(11)	0.215(19)	0.390(13)	0.400(11)	46.6(0.5)	221(9)
220	60	0.773(13)	0.185(11)	0.042(8)	0.249(23)	0.531(16)	0.220(9)	45.4(0.9)	200(8)
220	100	0.617(16)	0.229(8)	0.154(18)	0.251(22)	0.362(8)	0.387(23)	50.6(1.2)	109(10)
220	100	0.532(19)	0.373(15)	0.095(7)	0.252(21)	0.539(22)	0.209(13)	53.1(2.1)	97.3(7)
220	100	0.722(26)	0.123(11)	0.164(11)	0.217(11)	0.196(9)	0.567(9)	50.6(1.2)	128(5)
220	100	0.857(18)	0.143(18)	0.0(0)	0.206(22)	0.794(22)	0.0(0)	43.1(0.9)	143(6)
230	30	0.928(7)	0.051(8)	0.021(3)	0.344(4)	0.344(4)	0.312(4)	44.5(0.6)	534(17)
230	30	0.905(19)	0.078(18)	0.017(3)	0.378(11)	0.445(9)	0.177(3)	45.0(1.2)	535(20)
230	30	0.943(8)	0.026(3)	0.031(7)	0.387(7)	0.164(2)	0.450(5)	44.2(1.0)	554(17)
230	62	0.742(12)	0.176(11)	0.082(11)	0.238(12)	0.379(10)	0.383(8)	50.7(1.3)	234(9)
230	62	0.637(19)	0.296(11)	0.068(10)	0.279(10)	0.473(5)	0.248(7)	58.1(3.1)	248(11)
230	62	0.865(22)	0.052(9)	0.083(21)	0.257(10)	0.158(6)	0.584(8)	45.3(1.1)	251(8)
230	62	0.630(21)	0.332(15)	0.038(11)	0.281(12)	0.493(8)	0.227(7)	58.7(3.2)	249(11)
230	86	0.797(28)	0.085(12)	0.118(20)	0.253(20)	0.212(11)	0.533(14)	47.1(1.4)	167(6)
230	86	0.667(18)	0.209(10)	0.127(12)	0.293(20)	0.356(14)	0.350(20)	52.2(2.3)	130(8)
230	86	0.622(21)	0.283(18)	0.096(19)	0.278(19)	0.475(14)	0.247(9)	53.1(2.3)	131(9)
230	86	0.638(14)	0.283(11)	0.080(8)	0.268(30)	0.505(24)	0.226(13)	51.8(1.5)	148(8)
230	86	0.490(30)	0.420(28)	0.100(7)	0.274(26)	0.522(25)	0.195(10)	52.1(1.7)	140(9)
250	90	0.764(18)	0.106(12)	0.130(12)	0.400(21)	0.215(10)	0.385(18)	55.2(2.3)	157(11)
250	90	0.694(26)	0.216(24)	0.090(8)	0.400(24)	0.385(18)	0.215(11)	58.2(2.5)	146(10)
250	90	0.594(31)	0.327(28)	0.079(13)	0.425(24)	0.440(20)	0.135(9)	70.2(3.0)	131(10)
250	90	0.811(19)	0.189(19)	0.0(0)	0.368(12)	0.632(12)	0.0(0)	53.5(1.1)	179(10)
270	61	0.932(9)	0.028(3)	0.041(6)	0.635(21)	0.107(7)	0.262(18)	52.9(1.2)	275(11)
270	61	0.886(8)	0.087(6)	0.027(3)	0.624(20)	0.260(13)	0.136(10)	55.3(1.4)	265(10)

The numbers in the parentheses are the uncertainties in the simulation. For example, 0.873(15) means 0.873 \pm 0.015.



 $\textbf{Fig. 10.} \ \ \textbf{Ternary phase coexistence at 220 K and 60 bar.}$

approach introduced additional errors into their estimations, beyond the $5{\text -}15\,$ % errors already inherent in using the PR EOS for the binary systems.

The simulated results of this study are considerably different from their results. For example, our simulation at 220 K, of the system 72.2 % $\rm CO_2+12.3~\%CH_4+16.4~\%N_2$ (all in mole%) shows that it will homogenize at the molar volume of 50.6 cm³ whereas Thiéry et al. (1994b) find a molar volume of about 47 cm³ when they treated the system as a binary with composition.

To illustrate the potential applications of these simulations, the following hypothetical example of estimating the minimum formation temperature from a fluid inclusion observation is demonstrated. Micro-

thermometry allows the accurate determination of the homogenization temperature of a fluid inclusion, and Raman spectrometry provides a fairly accurate determination of the composition (Thiéry et al., 1994b). Suppose the fluid inclusion has a composition $x_{\rm CO2}=0.722,\,x_{\rm CH4}=0.123,\,$ and $x_{\rm N2}=0.164,\,$ and homogenizes to liquid at 220 K. When the vapor coexists with liquid for a fixed temperature, there are two degrees of freedom. Therefore, with the temperature and composition known, we can find the pressure and density by comparison of calculated phase equilibria with measured homogenization composition and temperature. Fig. 12 is a triangular isothermal phase diagram from our simulated data for T=220 K. The diamond symbol on the diagram is the system composition. When this point falls on a liquid/vapor coexistence line as a function of increasing pressure, the system will homogenize at certain pressure. In this illustration, this will occur for the 100 bar isobaric curve. This leads to a volume of 50.6 cm 3 per mole.

4. Discussion

The primary objective of this research is to demonstrate the Gibbs Ensemble Monte Carlo (GEMC) method as an efficient "computational experiment" for studying natural fluids. This approach is intended to complement existing experimental data and provide a deeper understanding of vapor-liquid phase equilibria at the molecular level. When compared to real experimental data, the GEMC method exhibits both similarities and differences, as well as distinct advantages and disadvantages.

Firstly, the GEMC computer simulation method closely mirrors the experimental process. From the initial setup, programming, compiling, and optimization, to running the program and collecting data, each step parallels a traditional experimental procedure. This similarity makes the GEMC method a powerful tool for studying molecular behavior.

The advantages of the GEMC method are significant. It allows researchers to observe molecules transitioning between phases and to simultaneously investigate various thermodynamic properties, including density, composition, and enthalpy. It seems easier to approach three phase equilibria, as indicated by the L_1L_2V equilibria.

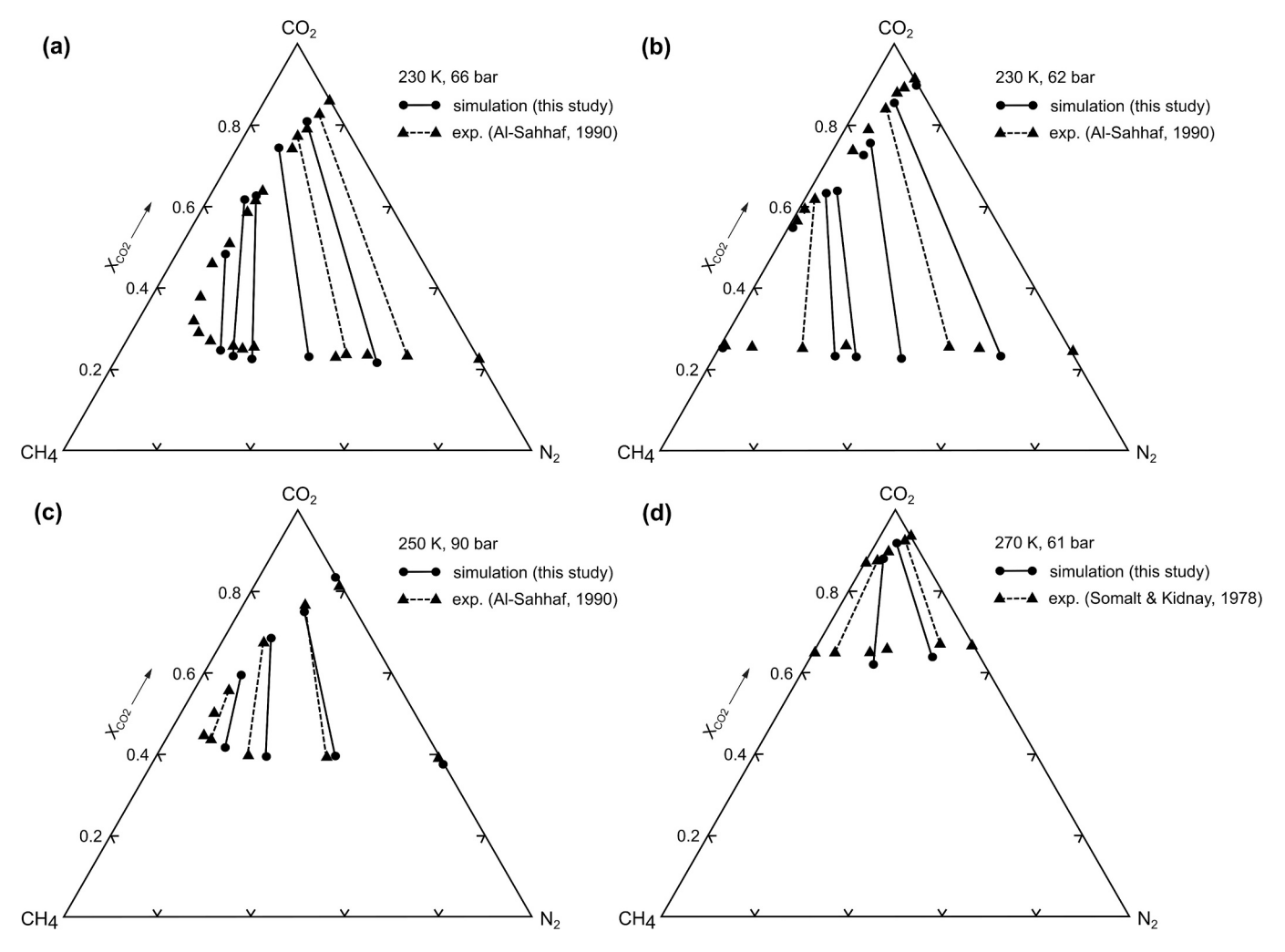


Fig. 11. Ternary phase coexistence at (a) 230 K and 66 bar, (b) 230 K and 62 bar, (c) 250 K and 90 bar, and (d) 270 K and 61 bar.

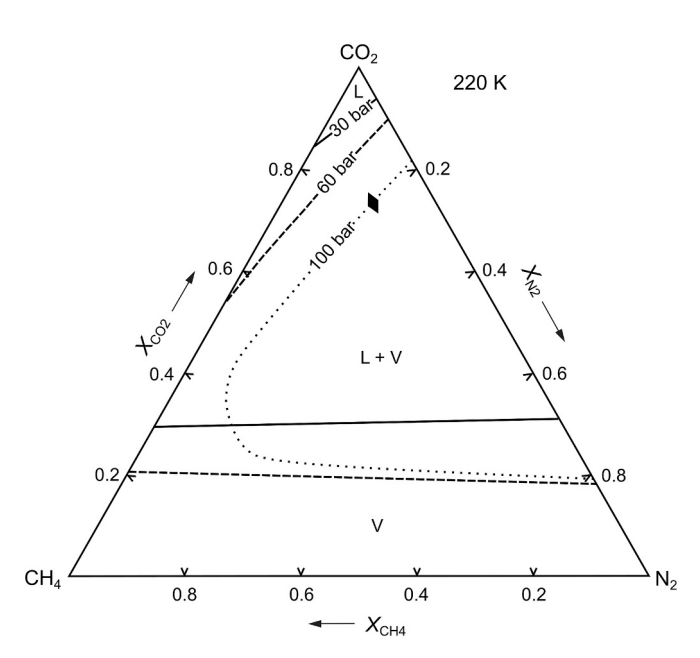


Fig. 12. The phase equilibria of the ternary $\rm CO_2\text{-}CH_4\text{-}N_2$ system at 220 K and various pressures (solid lines-30 bar, dashed lines-60 bar, and dot lines-100 bar).

However, the GEMC method also has notable disadvantages. The accuracy of the simulation results is highly dependent on the choice of molecular potentials. This dependency means that the reliability of the GEMC method is contingent upon the quality and appropriateness of the force fields used in the simulations. Therefore, while the GEMC method offers valuable insights, its results must be carefully interpreted in the context of the underlying molecular models. Another disadvantage is its very low insertion-acceptance ratio at low temperature of high densities, making it difficult to study high density fluid equilibrium.

Given the simplicity of the LJ potential, the closeness of the simulated results to experiments is remarkable, though there is room to improve potentials. In the future, multi-site potential or AI-based ab initio potential optimized by learning from high-fidelity quantum chemistry data can help create more accurate and transferable force fields for fluid simulations. The simulation results generated in this study serve as valuable supplements to experimental data, providing additional insights and expanding the knowledge base in this area.

The transferability of the GEMC computer simulation method to other systems depends on the choice of potential: The GEMC simulation is advantageous in certain *PT* regions, such as the critical region, where it is possible to outperforms parameterized EOS. However, this superiority is not universal across all regions. EOS can be broadly categorized into cubic EOS and virial EOS. While cubic EOS are highly accurate for calculating liquid-vapor phase equilibria of non-polar fluids, they tend to be less reliable for density calculations. In contrast, virial EOS can provide accurate density estimates but are less effective for vapor-liquid equilibrium (VLE) predictions. As demonstrated in this paper, the GEMC

simulation can simultaneously calculate both VLE and densities, offering a more comprehensive "computer experiment" approach.

The GEMC method enables the simulation of Liquid-Liquid-Vapor Equilibrium under low-temperature and low-pressure conditions. However, the reliability of these simulation results remains uncertain due to the scarcity of experimental data for comparison.

5. Conclusion

Results are presented for Gibbs Ensemble Monte Carlo (GEMC) simulations of fluid phase equilibrium in the $\rm CO_2\text{-}CH_4\text{-}N_2$ system. The model is based on an extremely simple two-body Lennard-Jones temperature-independent representation of the molecular interactions. Nevertheless, estimates of the coexistence compositions and densities in the unary, binary, and ternary systems obtained from the simulation are in general agreement with available data for a large range of temperatures and pressures.

In addition to presenting results for liquid-vapor coexistence, we explore gas-gas coexistence at high temperatures for the N_2 -CO $_2$ binary and liquid-liquid coexistence for the N_2 -CO $_2$, N_2 -CH $_4$, and CH $_4$ -CO $_2$ binaries. In agreement with prior assessments, the simulations predict that for the CH $_4$ -CO $_2$ and the N_2 -CH $_4$ binaries, there is a continuous critical line joining the endmember critical points in the PT plane. For the CO $_2$ -CH $_4$ binary and for lower temperatures the simulations support the existence of a three-phase vapor-liquid-liquid line intersecting a liquid-liquid (metastable liquid for CO $_2$) critical line at an upper critical endpoint, see Fig. 3a. For the N_2 -CO $_2$ the critical line coming out of the CO $_2$ cp does not end at the N_2 cp. However, we were not able to find a gas-gas critical line which joins the vapor-liquid critical line extending from the CO $_2$ cp. The three-phase vapor-liquid-liquid line intersects the extension of the vapor-liquid critical line emanating from the N_2 critical point.

While it is difficult to obtain highly accurate predictions of the various critical points and lines in these systems, bounds are reported. The remarkable agreement between the simulation outcomes and the available experimental data, despite the simplicity of the model, provides evidence of the accuracy of these simulations. Since the liquids have been observed in ternary fluid inclusions these simulations provide new information about their TP stability that may contribute to interpretation of fluid inclusions. Simulations of vapor-liquid coexistence in the ternary were also carried out. The predicted compositions of coexisting phases agree with data with accuracy near that of the experiments. The model may be used to estimate the pressure-volume relationships necessary for the interpretation of ternary fluid inclusion data.

CRediT authorship contribution statement

Zhenhao Duan: Writing – review & editing, Supervision, Methodology, Data curation, Visualization, Resources, Funding acquisition, Writing – original draft, Software, Investigation, Conceptualization, Validation, Project administration, Formal analysis. Nanfei Cheng: Writing – review & editing, Funding acquisition, Visualization, Data curation.

Declaration of competing interest

The authors declare that they have no known competing financial interests or personal relationships that could have appeared to influence the work reported in this paper.

Acknowledgments

We would like to thank Dr. John H. Weare for valuable discussions, and Mr. Haoran Sun for improving the quality of the figures. This research was financially supported by the Project of the Institute of Deep-sea Science and Engineering, Chinese Academy of Sciences (grant

number IDSSE-SJBS-202402), the Nanhai New Star Project (grant number NHXXRCXM202337) and the Innovational Fund for Scientific and Technological Personnel of Hainan Province (grant number KJRC2023C15).

Appendix A. Supplementary data

Supplementary data to this article can be found online at https://doi.org/10.1016/j.chemgeo.2025.122983.

Data availability

Data will be made available on request.

References

- Al-Sahhaf, T.A., Kidnay, A.J., Sloan, E.D., 1983. Liquid + vapor equilibria in the N₂ + CO₂ + CH₄ system. Ind. Eng. Chem. Fundam. 22, 372–380. https://doi.org/10.1021/i100012a004.
- Angus, S., Armstrong, B., Reukcc, M., 1976. International thermodynamic tables of the fluid state –3 carbon dioxide. In: International Union of Pure and Applied Chemistry Chemical Data Series. 16.
- Angus, S., Armstrong, B., Reukcc, M., 1978. International thermodynamic tables of the fluid state-5 methane. In: International Union of Pure and Applied Chemistry, Chemical Data Series, p. 18.
- Arai, Y., Kaminishi, G., Saito, S., 1971. The experimental determination of the PVTX relations for the carbon dioxide-nitrogen and the carbon dioxide-methane systems.
 J. Chem. Eng. Jpn. 113–122. https://doi.org/10.1252/jcej.4.113.
- Belonoshko, A., Saxena, S.K., 1991. A molecular dynamics study of the pressure-volume-temperature properties of supercritical fluids: II. CO₂, CH₄, CO, O₂, and H₂. Geochim. Cosmochim. Acta 55, 3191–3208. https://doi.org/10.1016/0016-7037 (91)90483-I.
- Brodholt, J., Wood, B., 1990. Molecular dynamics of water at high temperatures and pressures. Geochim. Cosmochim. Acta 54, 2611–2616. https://doi.org/10.1016/ 0016-7037(90)90247-I.
- Chen, Y., Chou, I.-M., 2022. Quantitative Raman spectroscopic determination of the composition, pressure, and density of CO₂-CH₄ gas mixtures. J. Spectrosc. 2022, 7238044. https://doi.org/10.1155/2022/7238044.
- Chi, G., Steele-Mcinnis, M., 2024. Fluid Inclusion Studies. Elsevier B.V. https://doi.org/ 10.1016/C2022-0-01146-6.
- Duan, Z., Møller, N., Weare, J.H., 1995. Molecular dynamics equation of state for nonpolar geochemical fluids. Geochim. Cosmochim. Acta 59, 1533–1538. https:// doi.org/10.1016/0016-7037(95)00059-9.
- Duan, Z., Møller, N., Weare, J.H., 1996. A general equation of state for supercritical fluid mixtures and molecular dynamics simulation of mixture PVTX properties. Geochim. Cosmochim. Acta 60, 1209–1216. https://doi.org/10.1016/0016-7037(96)00004-X.
- Duan, Z., Møller, N., Weare, J.H., 2000. Accurate prediction of the thermodynamic properties of fluids in the system H₂O–CO₂–CH₄–N₂ up to 2000 K and 100 kbar from a corresponding states/one fluid equation of state. Geochim. Cosmochim. Acta 64, 1069–1075. https://doi.org/10.1016/S0016-7037(99)00368-3.
- Duan, Z., Møller, N., Weare, J.H., 2003. Equations of state for the NaCl-H₂O-CH₄ system and the NaCl-H₂O-CO₂-CH₄ system: phase equilibria and volumetric properties above 573 K. Geochim. Cosmochim. Acta 67, 671–680. https://doi.org/10.1016/S0016-7037(02)01226-7.
- Duan, Z., Møller, N., Weare, J.H., 2004. Gibbs ensemble simulations of vapor/liquid equilibrium using the flexible RWK2 water potential. J. Phys. Chem. B 108 (52), 20303–20309.
- Faramawy, S., Zaki, T., Sakr, A.A., 2016. Natural gas origin, composition, and processing: a review. J. Nat. Gas Sci. Eng. 34, 34–54. https://doi.org/10.1016/j. ingse.2016.06.030.
- Gubbins, K., 1985. Theory and computer simulation studies of liquid mixtures. Fluid Phase Equilib. 20, 1–25. https://doi.org/10.1016/0378-3812(85)90018-4.
- Gubbins, K.E., Shing, K.S., Streett, W.B., 1983. Fluid phase equilibriums: experiment, computer simulation, and theory. J. Phys. Chem. 87, 4573–4585. https://doi.org/10.1021/j100246a009.
- Henley, H., Lucia, A., 2015. Constant pressure Gibbs ensemble Monte Carlo simulations for the prediction of structure I gas hydrate occupancy. J. Nat. Gas Sci. Eng. 26, 446–452. https://doi.org/10.1016/j.jngse.2015.05.038.
- Jin, G.X., Tang, S., Sengers, J.V., 1993. Global thermodynamic behavior of fluid mixtures in the critical region. Phys. Rev. E 47, 388–402. https://doi.org/10.1103/ PhysRevE 47, 388
- Kiselev, S.B., Friend, D.G., 1999. Revision of a multiparameter equation of state to improve the representation in the critical region: application to water. Fluid Phase Equilib. 155, 33–55. https://doi.org/10.1016/S0378-3812(98)00450-6.
- Kreglewski, A., Kenneth, R.H., 1983. Phase equilibria calculated for the systems N₂ + CO₂, CH₄ + CO₂ and CH₄ + H₂S. Fluid Phase Equilib. 15, 11–32. https://doi.org/ 10.1016/0378-3812(83)80020-X.
- Le, V.H., Caumon, M.C., Tarantola, A., Randi, A., Robert, P., Mullis, J., 2020. Calibration data for simultaneous determination of P-V-X properties of binary and ternary $\rm CO_2$ -CH₄-N₂ gas mixtures by Raman spectroscopy over 5–600 bar: Application to natural

- fluid inclusions. Chem. Geol. 552, 119783. https://doi.org/10.1016/j.
- Lee, B.I., Kesler, M.G., 1975. A generalized thermodynamic correlation based on three-parameter corresponding states. AICHE J. 21, 510–527. https://doi.org/10.1002/
- Ley-Koo, M., Green, M.S., 1981. Consequences of the renormalization group for the thermodynamics of fluids near the critical point. Phys. Rev. A 23, 2650–2659. https://doi.org/10.1103/PhysRevA.23.2650.
- Li, Y., Yu, Y., Zheng, Y., Li, J., 2012. Vapor–liquid equilibrium properties for confined binary mixtures involving CO₂, CH₄, and N₂ from Gibbs ensemble Monte Carlo simulations. Sci. China Chem. 55, 1825–1831. https://doi.org/10.1007/s11426-012-4724-5.
- Mao, S., Duan, Z., Hu, J., Zhang, D., 2010. A model for single-phase PVTx properties of CO₂-CH₄-C₂H₆-N₂-H₂O-NaCl fluid mixtures from 273 to 1273K and from 1 to 5000bar. Chem. Geol. 275, 148–160. https://doi.org/10.1016/j.chemgeo.2010.05.004.
- McGlashan, M.L., Schneider, G.M., 1978. High-pressure phase diagrams and critical properties of fluid mixtures. In: McGlashan, M.L. (Ed.), Chemical Thermodynamics. The Royal Society of Chemistry, pp. 105–146. https://doi.org/10.1039/ 9781847555830-00105.
- Pablo, J.D.E., Prausnitz, M., 1989. Phase equilibria for fluid mixtures from Monte-Carlo simulation. Fluid Phase Equilib. 53, 177–189. https://doi.org/10.1016/0378-3812 (89)80085-8.
- Panagiotopoulos, A.Z., 1987. Direct determination of phase coexistence properties of fluids by Monte Carlo simulation in a new ensemble. Mol. Phys. 61, 813–826. https://doi.org/10.1080/00268978700101491.
- Panagiotopoulos, A.Z., 1992. Direct determination of fluid phase equilibria by simulation in the Gibbs ensemble: a Review. Mol. Simul. 9, 1–23. https://doi.org/10.1080/08027029208048258
- Panagiotopoulos, A.Z., 2000. Monte Carlo methods for phase equilibria of fluids. J. Phys. Condens. Matter 12, R25–R52. https://doi.org/10.1088/0953-8984/12/3/201.
- Panagiotopoulos, A.Z., Quirke, N., Stapleton, M., 1988. Phase equilibria by simulation in the Gibbs ensemble. Mol. Phys. 63, 37–41. https://doi.org/10.1080/00268978800100361
- Peng, D., Robinson, D.B., 1976. A new two-constant equation of state. Ind. Eng. Chem. Fundam. 15, 59–64. https://doi.org/10.1021/i160057a011.
- Poling, B.E., Prausnitz, J.M., O'Connell, J.P., 2001. The Properties of Gases and Liquids, 5th edition. McGraw-Hill, New York.
- Roedder, E., 1984. Fluid inclusions. Rev. Mineral. 12.
- Sadus, R.J., 1999. Molecular simulation of the phase behaviour of ternary fluid mixtures: the effect of a third component on vapour-liquid and liquid-liquid coexistence. Fluid Phase Equilib. 157 (1999), 169–180. https://doi.org/10.1016/S0378-3812(99) 00049-7.
- Samson, I., Anderson, A., Marshall, D., 2003. Fluid Inclusions: Analysis and Interpretation. Mineralogical Association of Canada. https://doi.org/10.3749/ 9780921294672.
- Seitz, J.C., Blencoe, J.G., Joyce, D.B., Bodnar, R.J., 1994. Volumetric properties of CO₂-CH₄-N₂ fluids at 200°C and 1000 bars: a comparison of equations of state and experimental data. Geochim. Cosmochim. Acta 58, 1065–1071. https://doi.org/10.1016/0016-7037(94)90572-X
- Soave, G., 1993. 20 years of Redlich-Kwong equation of state. Fluid Phase Equilib. 82, 345–359. https://doi.org/10.1016/0378-3812(93)87158-W.

- Span, R., Wagner, W., 1996. A new equation of state for carbon dioxide covering the fluid region from the triple-point temperature to 1100 K at pressures up to 800 MPa. J. Phys. Chem. Ref. Data Monogr. 25, 1509–1596. https://doi.org/10.1063/ 1.555001
- Stryjek, R., Chappelear, P.S., Kobayashi, R., 1974. Low-temperature vapor-liquid equilibriums of nitrogen-methane system. J. Chem. Eng. Data 19, 334–339. https://doi.org/10.1021/je60063a023
- Sublett, D.M., Sendula, E., Lamadrid, H.M., Steele-MacInnis, M., Spiekermann, G., Bodnar, R.J., 2021. Raman spectral behavior of N₂, CO₂, and CH₄ in N₂–CO₂–CH₄ gas mixtures from 22°C to 200°C and 10 to 500 bars, with application to other gas mixtures. J. Raman Spectrosc. 52, 750–769. https://doi.org/10.1002/jrs.6033.
- Thiéry, R., Dubessy, J., 1996. Improved modelling of vapour-liquid equilibria up to the critical region. Application to the CO₂-CH₄-N₂ system. Fluid Phase Equilib. 121, 111–123. https://doi.org/10.1016/0378-3812(96)03029-4.
- Thiéry, R., van den Kerkhof, A.M., Dubessy, J., 1994a. vX properties of CH₄-CO₂ and CO₂-N₂ fluid inclusions: modelling for T. Eur. J. Mineral. 6, 753–772. https://doi.org/10.1127/eim/6/6/0753.
- Thiéry, R., Vidal, J., Dubessy, J., 1994b. Phase equilibria modelling applied to fluid inclusions: Liquid-vapour equilibria and calculation of the molar volume in the CO₂-CH₄-N₂ system. Geochim. Cosmochim. Acta 58, 1073–1082. https://doi.org/ 10.1016/0016-7037(94)90573-8.
- van den Kerkhof, A.M., 1990. Isochoric phase diagrams in the systems CO₂-CH₄ and CO₂-N₂: Application to fluid inclusions. Geochim. Cosmochim. Acta 54, 621–629. https://doi.org/10.1016/0016-7037(90)90358-R.
- van den Kerkhof, A.M., Frezzotti, M.L., Talarico, F., Berdnikov, N.V., 1993. Metastable phase transition in the system CO₂-CH₄-N₂ including immiscibility of the undercooled liquid (L1L2G): An example from granulites of the Wilson Terrane, North Victoria Land (Antarctica). In: ECROFI XII. European Current Research on Fluid Inclusions. Biennal Symposium, vol. 12, pp. 227–229. Warsaw 1993-06-13.
- van Konynenburg, P.H., Scott, R.L., 1980. Critical lines and phase equilibria in binary van der Waals mixtures. Philos. Trans. R. Soc. A 298, 495–540. https://doi.org/ 10.1098/rsta.1980.0266.
- Wagner, W., Span, R., 1993. Special equations of state for methane, argon, and nitrogen for the temperature range from 270 to 350 K at pressures up to 30 MPa. Int. J. Thermophys. 14, 699–725. https://doi.org/10.1007/BF00502103.
- Wegner, F.J., 1972. Corrections to scaling laws. Phys. Rev. B 5, 4529–4536. https://doi. org/10.1103/PhysRevB.5.4529.
- Yang, Y., Narayanan Nair, A.K., Sun, S., 2017. Molecular dynamics simulation study of carbon dioxide, methane, and their mixture in the presence of brine. J. Phys. Chem. B 121, 9688–9698. https://doi.org/10.1021/acs.jpcb.7b08118.
- Zhang, H., Chou, I.M., 2024. Raman spectroscopic characterization of the CO₂-N₂ gaseous system at 24–300°C and 2–40 MPa and applications. High Pressure Res. 44, 1–24, https://doi.org/10.1080/08957959.2023.2281953.
- Zhang, Z., Duan, Z., 2005. Prediction of the PVT properties of water over wide range of temperatures and pressures from molecular dynamics simulation. Phys. Earth Planet. Inter. 149, 335–354. https://doi.org/10.1016/j.pepi.2004.11.003.
- Zhang, J., Mao, S., Shi, Z., 2023a. A Helmholtz free energy equation of state of CO₂-CH₄-N₂ fluid mixtures (ZMS EOS) and its applications. Appl. Sci. 13, 3659. https://doi.org/10.3390/appl.3063659
- Zhang, L., Yang, Y., Yin, K., Liu, Y., 2023b. A review of GEMC method and its improved algorithms. Acta Geochim. 42, 409–434. https://doi.org/10.1007/s11631-023-00603-z.